Effect of NIP and PIN Architectures on the Performance of $FASnI_3$ Perovskite Solar Cells

Adrian Akbar Untoro[1,2], Rossyaila Matsna Muslimawati[3], Mohammad Kemal Agusta[4] and Muhammad Haris Mahyuddin[4,*]

[1]Master Program of Engineering Physics, Faculty of Industrial Technology, Institut Teknologi Bandung, Jl. Ganesha No. 10 Bandung 40132, Indonesia.
[2] Portfolio Department of PT PLN Nusantara Renewables, Jalan TB Simatupang No .18 Jakarta Selatan 12520, Indonesia
[3]Doctoral Program of Engineering Physics, Faculty of Industrial Technology, Institut Teknologi Bandung, Jl. Ganesha No. 10 Bandung 40132, Indonesia
[4]Quantum and Nano Technology Research Group, Faculty of Industrial Technology, Institut Teknologi Bandung, Jl. Ganesha No. 10 Bandung 40132, Indonesia
*Email: mahyuddin133@itb.ac.id

Abstract. This study explore the impact of NIP and PIN architectures on the performance of $FASnI_3$-based perovskite solar cells (PSCs) through simulations using the SCAPS-1D software. $FASnI_3$ is a promising material for PSCs due to its suitable bandgap, better thermal stability, and lower toxicity compared to Pb-based perovskites. The optimization of the NIP structure involves variations in donor density and the thickness of the $FASnI_3$ layer. A donor density in the form of a shallow density acceptor of 10^{17} cm^{-3} leads to optimal performance improvement. Comparisons between NIP and PIN configurations show that although the NIP architecture outperforms PIN with Spiro-OMeTAD as hotel transport layer (HTL) material, the choice of HTL significantly affects the efficiency of the PIN architecture. PTAA is identified as the best HTL for the PIN structure, offering higher efficiency. Additionally, the study also investigates the optimization of the capture cross-section value to 10^{-19}, resulting in maximum solar cell performance for all HTL material options. The efficiencies of solar cells with HTL materials PTAA, PEDOT:PSS, and Spiro-OMeTAD are 22.54%, 16.78%, and 4.58%, respectively, with Au electrodes.

Keywords: *perovskite solar cells, $FASnI_3$, NIP architecture, PIN architecture, hole transport layer, SCAPS-1D.*

1 Introduction

Concerns regarding climate change are further intensified by the large-scale consumption of fossil fuels, prompting the pursuit of sustainable, environmentally friendly, and cost-effective alternatives, such as renewable energy sources. Due to its abundant availability, solar energy is one of the most promising renewable energy sources, with the potential to meet energy needs. Solar cells have been developed to harness solar energy. Currently, in the commercial market, solar cells are dominated by silicon crystalline solar cells due

Received _____, Revised _____, Accepted for publication _____

to their relatively low production costs and reliable performance with power conversion efficiency (PCE) of up to 26.6% [1]. However, the Shockley-Queasier limit, according to the modern version, suggests that silicon-based cells have a maximum theoretical efficiency of 33% [2].

Perovskite solar cells (PSCs) have emerged as a promising alternative due to their lower production costs and environmentally friendly fabrication process [3]. However, perovskites encounter insurmountable challenges related to stability, especially when exposed to harsh conditions such as high humidity, heat, and UV light [4]. Additionally, lead-based perovskites ($MAPbI_3$, etc), despite their high efficiency, raise environmental and health concerns due to the toxicity of lead [5]. $FASnI_3$ has been introduced as a promising alternative as it exhibits a bandgap of 1.4 eV and offers better thermal stability and more durable performance compared to $CsSnI_3$. Nevertheless, $FASnI_3$ experiences issues related to Sn^{2+} oxidation to Sn^{4+}, though at a different level, and further optimization is required to enhance its overall efficiency [6].

PSCs can be classified into two categories based on the sequence of charge transport layers: regular negative-intrinsic-positive (NIP) and inverted positive-intrinsic-negative (PIN) structures. In both types, the light-absorbing perovskite layer is positioned between an electron transport layer (ETL) and a hole transport layer (HTL), as illustrated in Figure 1.

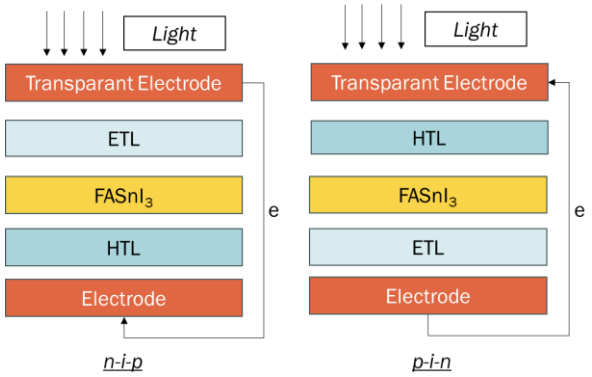

Figure 1 NIP and PIN architecture of PSC

PIN PSCs offer several advantages, including excellent operational stability, low-temperature fabrication, and compatibility with tandem devices. However, their efficiency is generally lower than NIP PSCs due to mismatched energy levels and poor interface quality at both the p-type and n-type contacts [7]. In the PIN-type PSCs, charge carriers—electrons and holes—are primarily generated near the front p-type contact. While holes can rapidly reach and be extracted at the adjacent p-type contact, electrons must diffuse across the entire perovskite layer

to reach the n-type contact for extraction as illustrated in Figure 2. To optimize charge extraction and minimize energy losses, the conduction properties of the perovskite layer should be tailored to the dominant carrier type in the device. Specifically, utilizing predominantly p-type or n-type perovskites is crucial for efficient charge extraction and reduced energetic barriers in PIN and NIP devices.

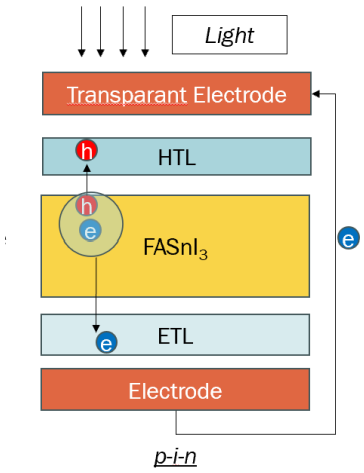

Figure 2 Generation of electron and hole in PIN architecture of PSC

In conventional PIN-type PSCs, materials like PTAA, PEDOT:PSS, and NiO_x are commonly used as p-type charge transport layers. However, organic HTLs are prone to significant degradation under light exposure, high temperatures, or moisture [8,9], and inorganic NiO_x tends to react with organic cations in the perovskite layer above it [10]. Additionally, the surface potential and conduction types of the HTLs influence the quality and properties of the as-deposited perovskite films. The charge-carrier mobility and energy levels of the hole transport materials determine the hole extraction efficiency of the device. Moreover, in the operation of PIN-type perovskite solar cells (PSCs), the HTLs are first passed through by incident light before the perovskite light-absorbing layer is reached. As a result, the optical properties of the HTL, such as refractive index and absorption coefficients, play a crucial role in determining the light absorption and photoelectric field distribution within the device [11].

In this study, we investigate PSC with $FTO/TiO_2/FASnI_3$/Spiro-OMeTAD/Au architecture and analyze the impact of the inverted PSC. In this work, SCAPS-1D is utilized to understand the effect of the inverted structure of PSCs. The layer thickness of the perovskite layer is also optimized with the variation of HTL materials. We found that the NIP structure showed superior performance, achieving a peak efficiency of 15.01% with an optimal shallow acceptor density

of 10^{17} cm^{-3}. Although the PIN architecture generally underperformed compared to NIP, careful selection of the HTL was shown to improve efficiency.

2 Methodology

SCAPS-1D software, a one-dimensional simulation software for modeling and simulating solar cell devices, was used for all calculations. Two architectures of PSCs model were used, that are FTO/TiO_2/$FASnI_3$/Spiro-OMeTAD/Au and inverted FTO/Spiro-OMeTAD/$FASnI_3$/TiO_2Au. First, the PSC model was optimized by varying the layer thickness of $FASnI_3$ between 1000 – 2000 nm and the Shallow Acceptor Density between 10^{12} - 10^{20} cm^{-3}. Secondly, the PIN (inverted PSCs) model was investigated. Finally, the study was conducted to evaluate the performance of PSC using a variation of HTLs material such as PEDOT:PSS and PTAA and layer thickness of $FASnI_3$. Several physical parameters derived from experimental data were utilized as summarized in Table 1 and 2.

Table 1 Material parameters in the simulation

Parameters	TiO_2	$FASnI_3$	ITO
Thickness(nm)	30 - 300	1000-2000	50
Bandgap (eV)	3.2	1.41	3.6
Electron affinity (eV)	4.1	4.2	4.5
Dielectric permittivity	55	8.2	8.9
CB effective density of states (cm^{-3})	1.0×10^{21}	1×10^{18}	2.2×10^{18}
VB effective density of states (cm^{-3})	2.0×10^{20}	1×10^{18}	1.8×10^{19}
Electron mobility (cm^2/Vs)	0.006	22	200
Hole mobility (cm^2/Vs)	0.006	22	80
Electron thermal velocity (cm/s)	10^7	10^7	10^7
Hole thermal velocity (cm/s)	10^7	10^7	10^7
Defect density, Nt [cm^{-3}]	10^{15} - 10^{21}	4.6×10^{16}	-
Shallow donor density, ND(cm^{-3})	10^{16} - 10^{22}	-	10^{21}
Shallow acceptor density, NA (cm^{-3})	-	10^{12} -10^{20}	-
Reference	[13]	[11]	[11]

Table 2 Material parameters of different HTL layers

Parameters	PTAA	PEDOT:PSS	Spiro - OMeTAD
Thickness (nm)	20	1000	200
Bandgap (eV)	3.2	2,2	3.5
Electron affinity (eV)	2.13	2.9	2.05
Dielectric permittivity	3	8.2	3
CB effective density of states (cm^{-3})	2.0×10^{18}	2.2×10^{15}	2.2×10^{18}
VB effective density of states (cm^{-3})	2.0×10^{18}	1.8×10^{18}	1.8×10^{19}
Electron mobility (cm^2/Vs)	0.001	0.022	0.0002
Hole mobility (cm^2/Vs)	0.001	0.0002	0.0002
Electron thermal velocity (cm/s)	10^7	10^7	10^7
Hole thermal velocity (cm/s)	10^7	10^7	10^7
Defect density, Nt [cm^{-3}]	10^{15}	10^7	10^{15}
Shallow donor density, ND(cm^{-3})	-	-	-
Shallow acceptor density, NA (cm^{-3})	1.0×10^{22}	1.0×10^{19}	1.0×10^{16}
Reference	[12]	[11]	[11]

3 Results and Discussion

3.1 Pre-Optimization of the Model

Before initiating the investigation of NIP and PIN, an optimization of the NIP structure was first carried out with respect to shallow acceptor density (doping density) of the $FASnI_3$, defect of $FASnI_3$ and thickness of $FASnI_3$. First, an optimal shallow acceptor density for $FASnI_3$ is investigated.

Referring to the simulation below as shown in Figure 3 we observe that as the shallow acceptor density varied from 10^{12} to 10^{20} cm^{-3}, there is a gradual improvement in V_{oc}, J_{sc}, fill factor (FF), and overall efficiency (ETA). This trend indicates enhanced charge carrier collection and reduced recombination losses. However, at a density of 10^{17} cm^{-3}, there is a significant increase in all performance parameters, suggesting an optimal balance between carrier concentration and mobility. Beyond this point, at densities of 10^{18} cm^{-3} and higher, the performance begins to decline, likely due to increased recombination and scattering effects.

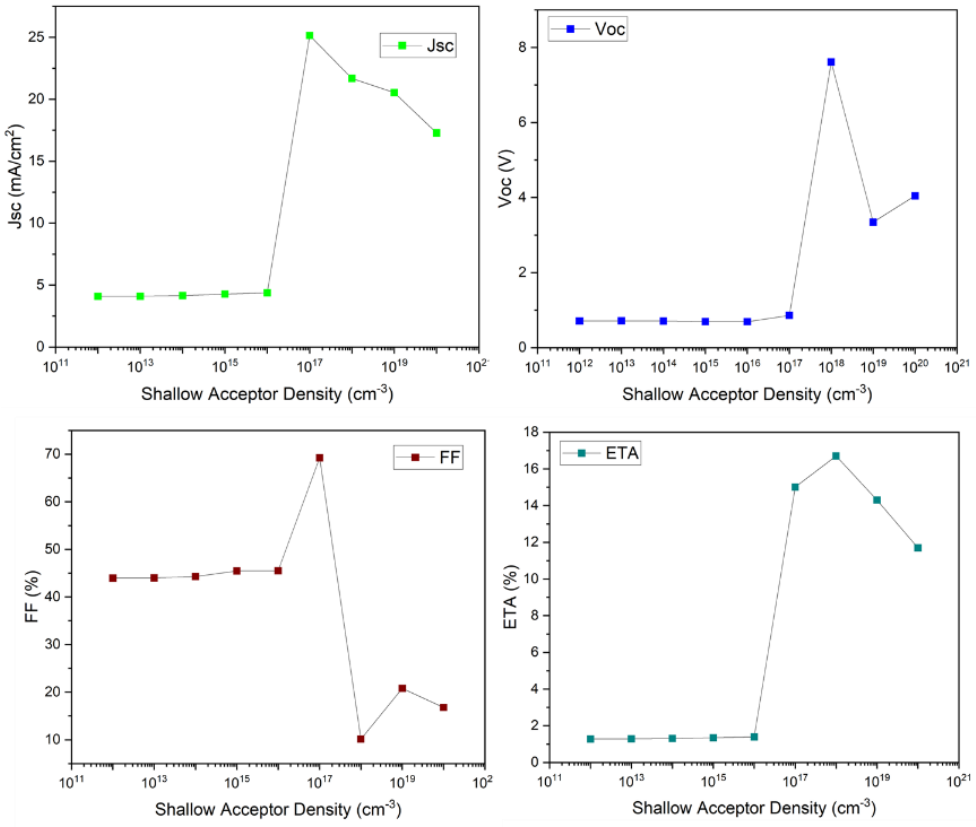

Figure 3 Simulation Result of Shallow Acceptor Density

After the optimum doping density was selected then the variation of capture cross section for electron and hole was conducted. The provided data in Figure 4 illustrates how the defect of absorbent especially the variations in the capture cross section of electron and hole impact key performance parameters such as open-circuit voltage (V_{oc}), short-circuit current density (J_{sc}), fill factor (FF), and power conversion efficiency (ETA).

As the capture cross section decreases from 10^{-15} to 10^{-19} cm^2, there is a notable increase in V_{oc}, $J_{sc,}$ and ETA. This trend suggests that smaller capture cross-sections are associated with reduced recombination rates, allowing for more efficient charge carrier collection and higher overall device performance. Specifically, V_{oc} increases significantly from 0.8606 V to 2.86 V, indicating improved separation of charge carriers and reduced recombination losses. Similarly, J_{sc} shows a steady rise, reflecting enhanced charge carrier generation and collection.

However, the fill factor (FF) exhibits a different trend, initially decreasing as the capture cross section decreases. This decline in FF can be attributed to increased series resistance and potential losses in the charge transport layers, which become more pronounced at smaller capture cross sections. Despite this, the overall efficiency (ETA) continues to improve, reaching a maximum of 23.18% at a capture cross section of 10^{-19} cm^2, due to the significant gains in V_{oc} and J_{sc}.

In summary, optimizing the capture cross-section is essential for maximizing the performance of perovskite solar cells. Smaller capture cross sections generally lead to higher V_{oc}, J_{sc}, and overall efficiency, although careful consideration must be given to the fill factor and potential resistive losses.

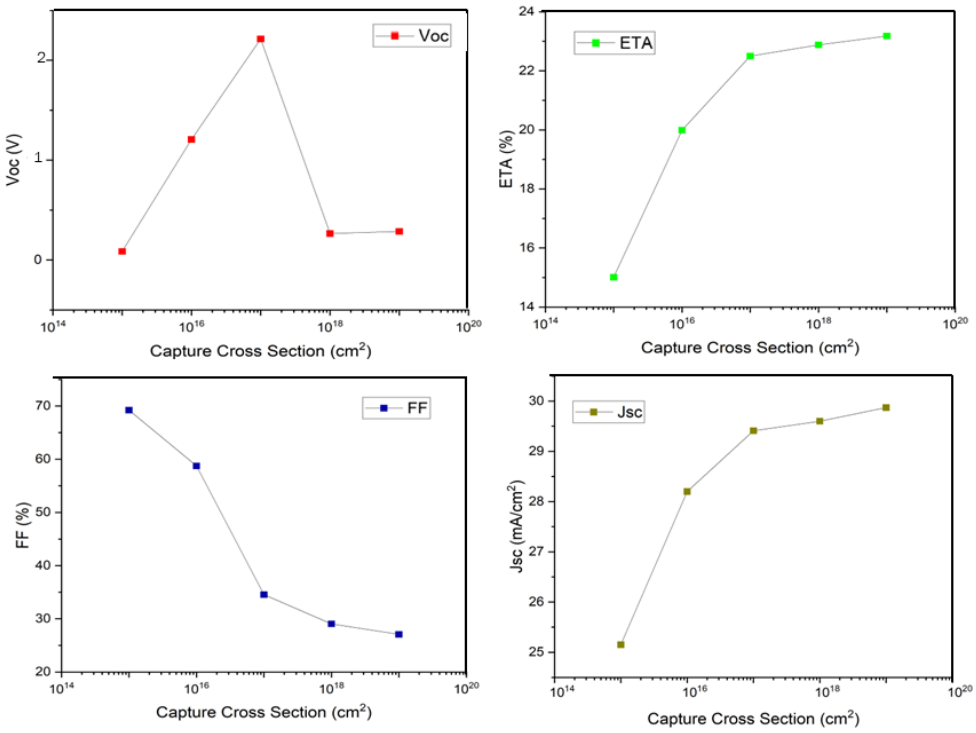

Figure 4 Simulation Result of Capture Cross Section Variation

Furthermore, the provided data in Figure 5, illustrates how variations in the thickness of $FASnI_3$ impact key performance parameters. Referring to the simulation, we concluded that the power conversion efficiency (ETA) shows a slight increase from 14.91% to 15.01% as the thickness increases from 1000 nm to 1400 nm, after which it stabilizes around 15.01%. This indicates that the

optimal thickness for maximizing efficiency is around 1400 nm, where the balance between photon absorption and recombination losses is most favorable.

In summary, while increasing the thickness of the $FASnI_3$ layer can slightly improve Jsc and ETA, the optimal thickness appears to be around 1400 nm. Beyond this point, the benefits of increased thickness are marginal, and further increases may lead to diminishing returns due to enhanced recombination losses.

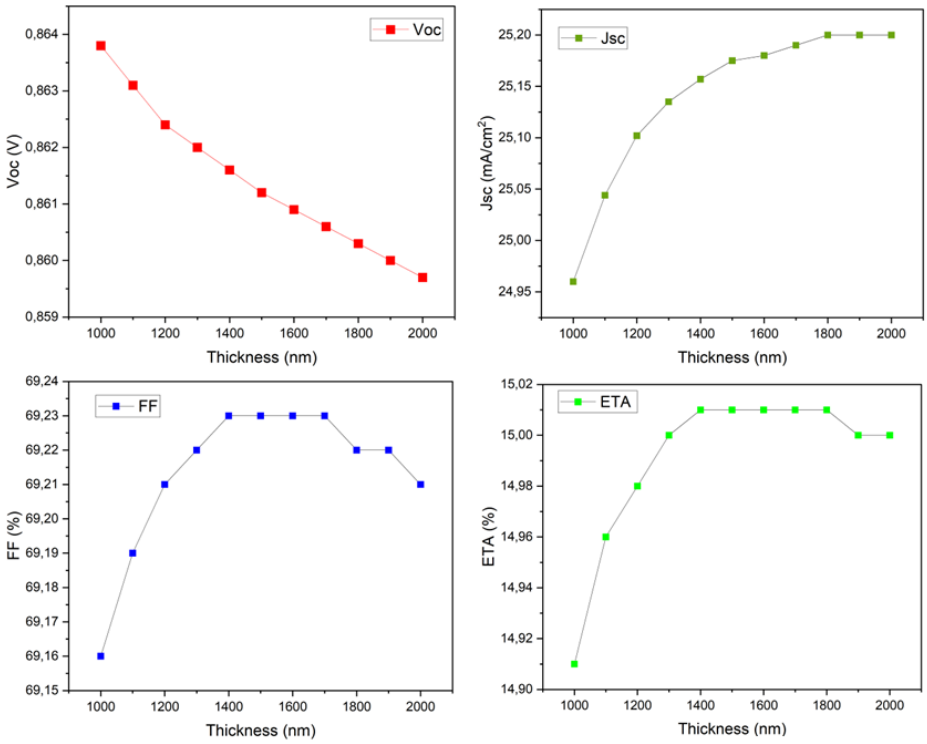

Figure 5 Simulation Result of $FASnI_3$ thickness

3.2 The Comparison between NIP and PIN Layer Architecture on PSC Performance

Subsequently, when the layer structure was modified from the previous NIP architecture to a PIN architecture, with the architecture as shown in Figure 5 below, adjustments were made. Based on the results obtained, assuming the transparent electrode was implemented as modified front contact, the efficiency (ETA) was only achieved at 0.12%.

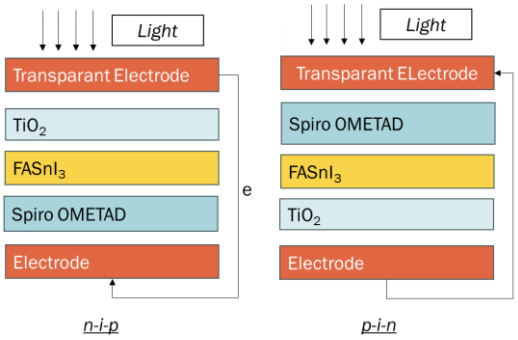

Figure 6 PSC Device Architecture and Materials Selection

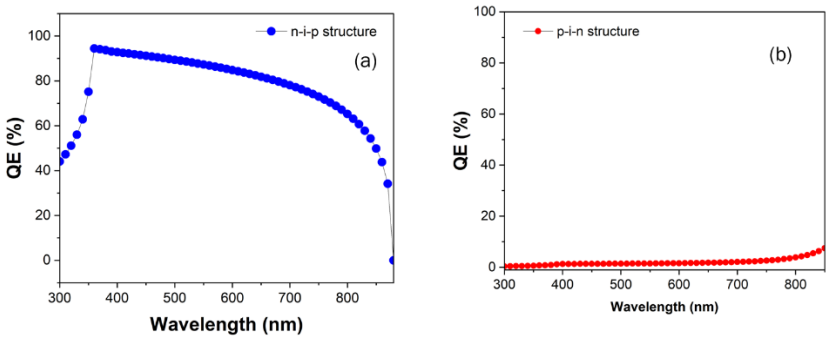

Figure 7 QE Curve for (a) NIP architecture and (b) PIN architecture

Referring to Figure 7 above, an optimum QE of over 80% is achieved in the visible light wavelength range of 360 to 670 nm for NIP architecture, and there is no visible light wavelength for PIN architecture.

The modification from the NIP architecture to the PIN architecture significantly reduces efficiency. In the PIN architecture, the n-type electron transport layer (TiO_2) is in direct contact with the p-type perovskite layer. This configuration leads to an enlarged energetic interfacial barrier for electron extraction at the n-type interface, which hinders the efficient transfer of electrons from the perovskite layer to the TiO_2 layer.

Additionally, this direct contact increases non-radiative charge recombination, where electrons and holes recombine without emitting photons, resulting in energy loss. These factors combined significantly reduce the efficiency of the solar cell in the PIN architecture compared to the NIP architecture, where such barriers and recombination losses are minimized

3.3 Effect of HTL on PIN PPV Performance

The HTL is crucial to the performance of perovskite solar cells in the PIN structure due to its role in efficient hole extraction and transport, energy level alignment with the perovskite layer, and overall cell stability. Therefore, it is critical to identify the HTL material to achieve optimal performance with the $FASnI_3$-PIN structure, as shown in Figure 8.

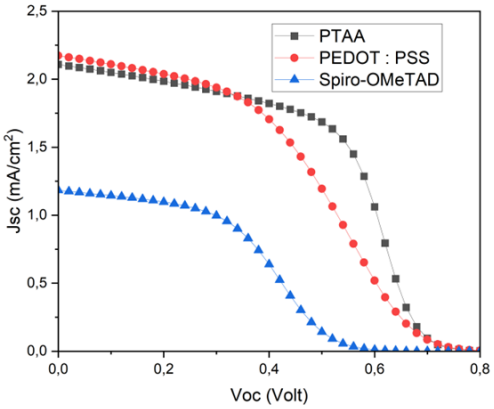

Figure 8 JV Curve for (a) PIN (Spiro-OMeTAD), (b) PIN (PEDOT : PSS) and (c) PIN (PTAA)

Based on the simulation results shown in Figure 8 above, in general, the performance of PIN-based perovskite solar cells with Spiro-OMeTAD as the HTL material shows a V_{oc} of 0.8145 V, J_{sc} of 1.183 mA/cm², FF of 31.87%, and ETA of 0.31%. Meanwhile, the use of PEDOT:PSS resulted in the following performance: V_{oc} of 0.8236 V, J_{sc} of 2.173 mA/cm², FF of 38.20%, and ETA of 0.68%.

However, the use of PTAA as the HTL material resulted in slightly better performance, with a V_{oc} of 0.8190 V, J_{sc} of 2.108 mA/cm², FF of 49.23%, and ETA of 0.85%. The transition from NIP to PIN structure does not automatically result in performance improvement.

PTAA is the best HTL material for PIN perovskite solar cells because PTAA has better hole mobility, which impacts the efficiency of charge transport in the device. Compared to Spiro-OMeTAD and PEDOT:PSS, the hole mobility values for each material are 0.001 cm²/Vs for PTAA, 0.0002 for Spiro-OMeTAD, and PEDOT:PSS, respectively.

Overall, the performance of PIN perovskite solar cells with HTL material variations such as Spiro-OMeTAD, PEDOT:PSS, and PTAA has not yet resulted

in good solar cell performance, so optimization is needed to improve the performance of PIN perovskite solar cells.

Additionally, simulations were conducted to observe the effect of defects (capture cross section) on FF and V_{oc}. Based on the results obtained, it was found that the same trend also occurred for FF and V_{oc}, namely the higher the value of the defect influence (capture cross section), the higher the values of FF and V_{oc}. However, there was a decrease in FF value at a defect value of 10^{-19} specifically for PTAA material, but at the same time, there was a change in V_{oc} value to 1.0351 V from the previous 0.8372 V at a defect value of 10^{-18}, resulting in a smaller FF value because FF is the ratio of P_{max} to the product of V_{oc} and J_{sc}.

Overall, the highest performance values for V_{oc}, J_{sc}, FF, and ETA are 1.0351 V, 31.24142 mA/cm², 69.69%, and 22.54%, respectively, using PTAA as the HTL material. Meanwhile, the performance values for V_{oc}, J_{sc}, FF, and ETA for Spiro-OMeTAD material are 0.8196 V, 13.321 mA/cm², 41.91%, and 4.58%, respectively.

4 Conclusion

This study examined the influence of NIP and PIN architectures on the performance of $FASnI_3$-based perovskite solar cells through simulations. The NIP structure showed superior performance, achieving a peak efficiency of 15.01% with an optimal shallow acceptor density of 10^{17} cm^{-3}. Although the PIN architecture generally underperformed compared to NIP, careful selection of the HTL was shown to improve efficiency. Among the tested HTLs, PTAA emerged as the best option for the PIN architecture. These findings highlight the importance of optimizing material properties and architectures to achieve higher efficiency in $FASnI_3$-based perovskite solar cells, with PTAA playing a critical role in improving the performance of the PIN configuration. Further research into material interfaces and stability is essential for advancing PSC technology.

References

[1] Ru, X., Yang, M., Yin, S., Wang, Y. et all, D., Silicon Heterojunction solar cells achieving 26,6% efficiency on commercial-size p-type silicon wafer, *Joule,* vol. 8, pp. 1092-1104, April 2023.

[2] Zanatta, A.R., The Shockey – Queisser limit and the conversion efficiency of silicon based colar cells, Optics, Vol. 9, 2022.

[3] Roy, P., Ghosh, A., Barclay, F., Khare, A., Cuce, E., Coatings, Vol 12, pp. 1809, 2022

[4] Lv, Y., Zhang, H., Liu, R., Sun, Y., Huang, W., Composite encapsulation enabled superior comprehensive stability of perovskite solar cells, ACS Appl. Mater. Interfaces, Vol 12, 2020.
[5] Yang, W.S., Noh, J.H., Jeon, J., Kim, Y.C., Ryu, S., Seo, J.,Seok, I., Science, Vol 348, pp. 1234, 2015.
[6] Abdelaziz, S., Zekry, A., Shaker, A., Ebrahim, M.A., Opt Mater, Vol 101, 2020
[7] Zhang, H., Park N.G., Progress and issues in PIN type perovskite solar cells, DeCarbon, Vol 3, 2024.
[8] Cameron, J., Skabara,P.J., The damaging effects of the acidity in PEDOT:PSS on semiconductor device performance and solutions based on non-acidic alternatives, Mater, Horiz, Vol 7, pp. 1759-1772, 2020, https://doi.org/10.1039/c9mh01978b.
[9] Sendner, M., Trollman, J., Pucci, A., Dielectric function and degradation process of poly (triarylamine) (PTAA), Orang. Electron, Vol 15, pp. 2959-2963, 2014, https://doi.org/10.1016/j.orgel.2014.08.037.
[10] Zhang, H., Toudert, J., Optical Management for efficiency enhacement in hybrid organic-inorganic lead halide perovskite solar cells, Sci Technol. Adv. Matter, Vol 19, pp. 411-424, 2018.
[11] Hosen, A., Mian, M.S., Ahmed, S.R.A, Improving the Performance of Lead – Free $FASnI_3$, - Based Perovskite Solar Cell with Nb2O5 as an Electrin Transport Layer, Advances Theory and Simulations, Vol 6, 2023.
[12] Ravinshankar, S., Liu, Z., Rau, U., Kirchartz, T., Multilayer Capacitances : How Selective Contact Affect Capacitance Measurement of Perovskite Solar Cells, PRX Energi, Vol 1, 2022
[13] Hossain, M.K., Numerical Analysis in DFT and SCAPS-1D on the Influence of Different Charge Transport Layers of $CsPbBr_3$ Perovskite Solar Cells , Energy Fuels,37,6078-6098, 2023.

Acknowledgment

The authors are grateful to PT. PLN (Persero) and PT PLN Nusantara Renewables for the financial and scholarship support provided throughout this research. The authors also acknowledge Professor Marc Burgelman from the University of Gent for providing and allowing us to utilize the SCAPS-1D simulation program.